Pergamon International Journal of Machine Tools & Manufacture 39 (1999) 751–769

INTERNATIONAL JOURNAL OF MACHINE TOOLS & MANUFACTURE DESIGN, RESEARCH AND APPLICATION

Basic geometric analysis of 3-D chip forms in metal cutting. Part 1: determining up-curl and side-curl radii

A. Kharkevich, Patri K. Venuvinod*

Department of Manufacturing Engineering and Engineering Management, City University of Hong Kong, Tat Chee Avenue, Kowloon, Hong Kong

Received 8 May 1998

Abstract

The works of Nakayama et al. represent the prevailing view on how the geometry of 3-D helical chip relates to the radii of its up-curl and side-curl. The view is re-examined in this paper and it is shown that the corresponding definitions of the radii are ambiguous. Six sets of alternative hypothetical definitions of up-curl and side-curl radii, which are consistent and plausible when examined from the viewpoints of 2-D up-curl and side-curl, are identified and the respective expressions are derived from a geometric analysis of 3-D chip. The hypotheses are tested using six criteria. It is found that the expressions for the radii of up-curl and side-curl proposed by Nakayama et al. do not satisfy one of the criteria whereas a new solution satisfies all the criteria. Part 2 extends the 3-D geometric analysis and discovers a number of new implications.

Keywords: Up-curl; Side-curl; Chip forms; Metal cutting; Helical chip

Nomenclature

A_H	Axis of **H**
A_{Hr}	projection of A_H on P_r
e	normal distance between A_{Hr} and axis X; distance between points O_{Hr} and O
f	distance between O_H and O_{Hr}
H	helical path generated by the chip particle at point O
$\mathbf{H}^{xy}$, $\mathbf{H}^{yz}$, $\mathbf{H}^{zx}$	projections of helix **H** on planes XY, YZ, and ZX respectively

* Corresponding author. Tel.: 852-2788-8400; Fax: 852-2788-8423; E-mail: mepatri@cityu.edu.hk

0890-6955/99/$ - see front matter
PII: S0890-6955(98)00065-0

$\mathbf{H}^{x_v y_v}$, $\mathbf{H}^{y_v z_v}$, $\mathbf{H}^{z_v x_v}$	projections of helix **H** on planes $X_V Y_V$, $Y_V Z_V$, and $Z_V X_V$ respectively
l_c	tool-chip contact length measured in a direction normal to the cutting edge
O	an arbitrary point on the TCSL
O_H	point at which the line passing through O in a direction normal to A_H meets A_H
O_{Hr}	projection of O on A_{Hr}
p	pitch of helical chip
P_r	tool rake plane
$[\mathbf{R_H}]$	transformation matrix from system XYZ to system $X_H Y_H Z_H$
$[\mathbf{R_V}]$	transformation matrix from system XYZ to system $X_V Y_V Z_V$
t	time measured from the moment the chip particle at O leaves the TCSL
TCSL	tool chip separation line
$\mathbf{V}_c$	velocity of chip particle at O (assumed to lie on P_r)
X, Y, Z	right-handed Cartesian axes centred at O such that X is parallel to A_{Hr}, Z is positively directed outward from the tool rake face and Y is perpendicular to A_{Hr} while being parallel to P_r
X′,Y′,Z′	right-handed Cartesian axes centred at O_H and directed parallel to axes X, Y, and Z respectively
X_H,Y_H,Z_H	right-handed Cartesian axes centred at O_H such that X_H is directed from O_H to O and Z_H is directed along $\boldsymbol{\omega}$
X_V, Y_V, Z_V	right-handed Cartesian axes centred at O such that Y_V is directed as $\mathbf{V}_c$, Z_V is positively directed outward from the tool rake face and X_V is parallel to P_r
X_V', Y_V', Z_V'	right-handed Cartesian axes centred at O_H such that the axes are directed parallel to axes X_V, Y_V, and Z_V respectively
$\Delta\psi$	angle between the major cutting edge (assumed to be straight) and TCSL
η_c	chip flow angle: angle between $\mathbf{V}_c$ and the normal to the cutting edge in P_r
η	angle between $\mathbf{V}_c$ and axis Y
$\boldsymbol{\kappa}$	vector of curvature of helix **H** at point O
θ	angle between A_H and A_{Hr}
$\boldsymbol{\rho}$	position vector of a particle of **H** at point O joining O_H to O
ρ_3	the third radius of chip curl complementing ρ_u and ρ_s that may exist under some definitions of ρ_u and ρ_s when the chip form is 3-D
ρ_s	radius of chip side-curl
ρ_u	radius of chip up-curl
$\rho^{\omega_{x'}}$, $\rho^{\omega_{y'}}$, $\rho^{\omega_{z'}}$	radii of rotation of the chip particle at O about axes X′, Y′, and Z′ respectively
$\rho^{\omega_{x_v'}}$, $\rho^{\omega_{y_v'}}$, $\rho^{\omega_{z_v'}}$	radii of rotation of the chip particle at O about axes X_V', Y_V', and Z_V' respectively
ρ_{Hxy}, ρ_{Hyz}, ρ_{Hzx}	radii of curvature of $\mathbf{H}^{xy}$, $\mathbf{H}^{yz}$ and $\mathbf{H}^{zx}$ respectively
$\rho_{Hx_vy_v}$, $\rho_{Hy_vz_v}$, $\rho_{Hz_vx_v}$	radii of curvature of $\mathbf{H}^{x_v y_v}$, $\mathbf{H}^{y_v z_v}$ and $\mathbf{H}^{z_v x_v}$ respectively
$\boldsymbol{\omega}$	angular velocity of rotation of the chip particle at O about helix axis A_H

Scalars are presented in regular font. If a vector corresponding to a scalar exists, it is represented by a similar symbol in bold font. The presence of x, x′, x_H, x_V, y, y′, y_H, y_V, z, z′, z_H or z_V in the suffix of a symbol indicates that the symbol refers to the component of that vector along the specific axis.

1. Introduction

The need for periodical manual removal of entangled chips from the cutting zone continues to be a major hurdle in the realisation of unmanned machining of metals. Machining industry currently relies on cutting inserts with appropriate chip formers (bumps and troughs on the rake surface) to solve the problem of chip breaking. However, in practice, each chip former design is found to be effective only in a narrow range of cutting situations. Further, owing to the absence of a systematic theory of chip form development, the design of these chip formers has remained an experimental art. The result has been an unnecessary proliferation of chip former designs. More recently, it has been suggested that it should be possible to achieve active chip control by controlling the location and orientation of an obstruction type chip former relative to the cutting edge in response to the chip form detected by a set of on-line sensors [1]. However, a prerequisite to the success of this approach is the availability of a systematic method for decomposing the geometry of a given chip form into a set of basic elements which can be related in a meaningful manner to the process of chip formation itself.

It is generally accepted that initially continuous chips are born curled and may subsequently break because of forces arising from an encounter with an obstacle (e.g. a tool or work surface) external to the chip formation zone. When the external forces are light, they merely modify the deformation pattern within the chip formation zone which, in turn, modifies the chip form as the chip leaves the cutting zone. Such a chip may be viewed as *lightly obstructed*. The present paper is confined to the analysis of such chips and unobstructed chips. When the external forces are strong, the deformation pattern within the chip formation zone is unable to adapt and the chip may experience further plastic deformation (or, even, breaking) outside the chip formation zone. Clearly, the geometry of the chip during the lightly loaded phase determines the possibility and nature of chip breaking. The majority of unobstructed or lightly obstructed chip forms obtained in continuous cutting operations such as turning are particular cases of 3-D helical chips. Thus, according to the popular chip form classifications such as those developed by Spaans [2] and ISO [3], chip types such as straight ribbon, tubular, corkscrew (washer) and conical helical chips are all particular cases of 3-D helical chip. Other chip types such as spiral, and arc chips can be considered as helical chips whose progression has been unsteady or arrested due to chip breaking respectively. Hence, while analysing chip forms, it is essential to have a logically consistent view of the mapping between the 3-D and 2-D manifestations of helical chip forms.

The work of Nakayama et al. [4,5] seems to represent the currently reigning paradigm concerning the geometric analysis of 3-D chip forms. These authors note that "basically the chip has a screw surface". They represent each helical trajectory, **H**, on this screw surface in terms of its radius, ρ, pitch, p, and the angle, θ, between the axis of the helix and the tool rake plane (see Fig. 1a). Further, they suggest that the geometric form of the chip prior to its breaking is completely determined by the velocity and curl states of the chip at the moment the chip leaves the tool-chip separation line (TCSL).

These velocity and curl states are in turn determined by the complex deformation patterns experienced by the work/chip material as it passes through the primary and secondary deformation zones prior to arriving at the TCSL. Thus the TCSL represents the boundary between the worlds of chip form analysis and chip formation analysis. Fig. 2 (adapted from [4]) illustrates the location and orientation of the TCSL in a turning operation. Generally speaking, the TCSL is not parallel to the cutting edge. No complete model for estimating the angle, $\Delta\psi$, between the TCSL and the cutting edge is yet available. When $\Delta\psi \neq 0$, the distance between the TCSL and the cutting edge (i.e. the tool-chip contact length, l_c) is not uniform. A non-uniform contact length suggests a non-uniform chip velocity across chip width. Greater this non-uniformity, greater is the side-curl of the chip. A review of literature on chip formation reveals that, although there have been many investigations related to l_c when it is constant, the more general case of non-uniform l_c has not yet been studied satisfactorily. This means that, in most cases, we do not have the means of estimating either the orientation or the location of the TCSL. Consider now our ability to estimate the angular deviation, η, of the chip velocity from the normal to the TCSL. It follows from Fig. 2 that $\eta = \eta_c - \Delta\psi$ [4,5] where η_c is the chip flow angle with respect to the cutting edge. While much literature exists with respect to η_c, there is no solution available for estimating $\Delta\psi$. Hence, it continues to be problematic to estimate η. It therefore appears that there are two essential tasks

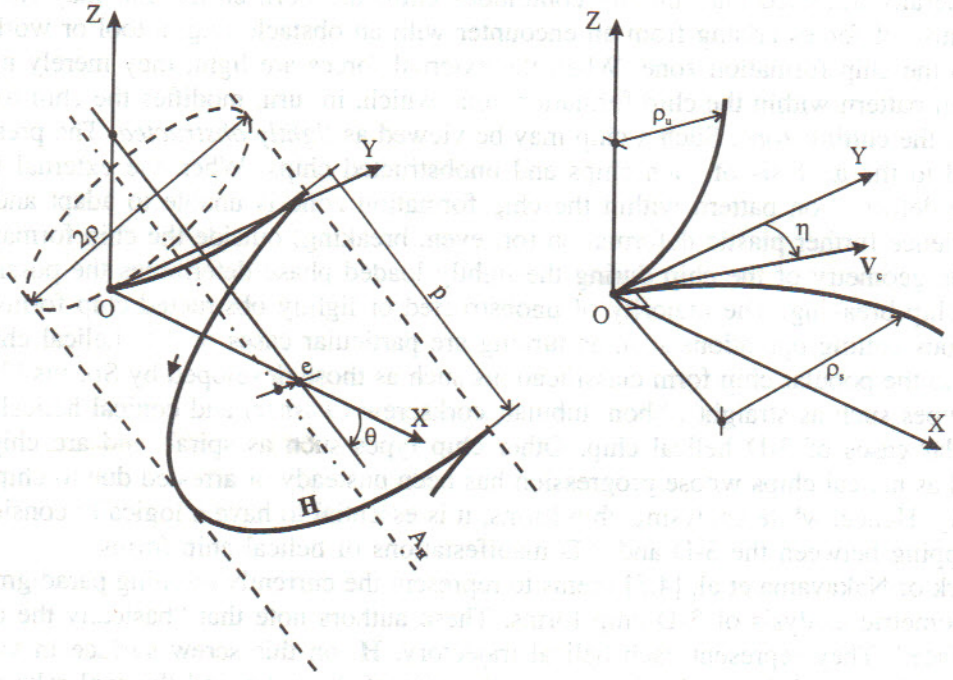

(a) Chip helix

(b) Orthogonal circular arcs in XOY and YOZ planes

Fig. 1. Helix as a compound of two orthogonal circular arcs (adapted from Nakayama and Arai [5]).

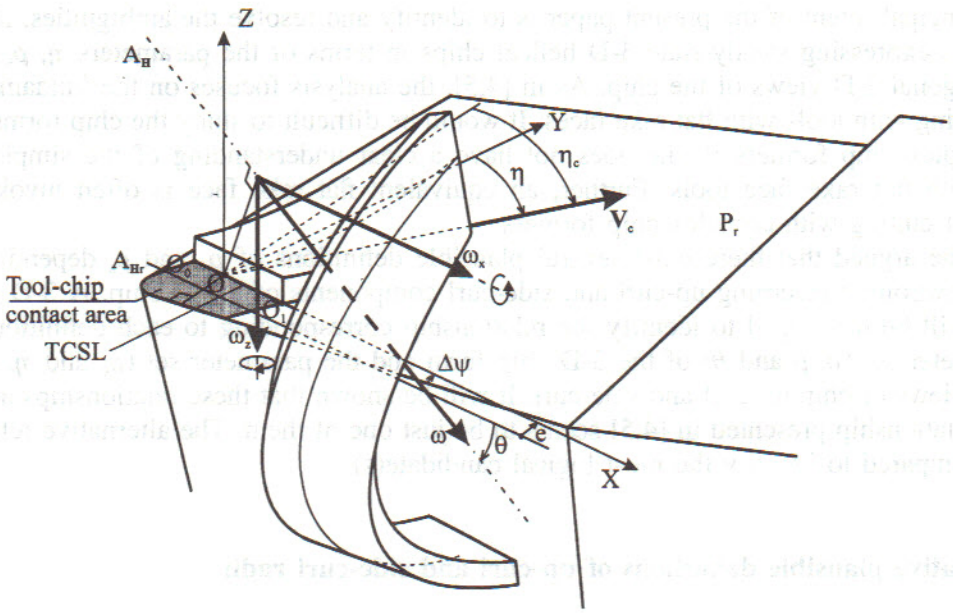

Fig. 2. TCSL in turning (adapted from Nakayama and Ogawa [4]).

in chip analysis. The first concerns the determination of the parameters of the TCSL (such as its location and the velocities of the chip particles along that line) from the viewpoint of the world of chip *formation* that manifests *before* the chip has arrived at the TCSL. The second task concerns how one may connect the parameters of the TCSL to the chip form that develops *after* the chip has left the TCSL and has entered the world of chip *form* analysis. While both these tasks are important, the present paper will focus on the second task. The solution of the second task is expected to open up new ways of addressing the first task.

A problem arising in the mapping between the 3-D and 2-D manifestations of helical chip forms is that, whereas chip form analyses need to be 3-D, almost all our present knowledge concerning chip form has been represented in terms of two orthogonal 2-D states of chip: pure (i.e. unmixed with another curling) up-curled chip and pure side-curled chip. For instance, recognising their dominance in the literature on chip formation, Nakayama et al. [4,5] have utilised the concepts of chip flow direction represented by angle η, the radius of side-curl, ρ_s, and the radius of up-curl, ρ_u, while attempting to express the 3-D chip form parameters ρ, p and θ. Note that ρ_s, η and ρ_u are essentially concepts related to two orthogonal 2-D states (see Fig. 1b).

It should be clear from the above that we are faced with the task of characterising a 3-D phenomenon from information concerning its *two* orthogonal 2-D views. Experience shows that one should generally expect ambiguities when one tries to map from two 2-D views to a 3-D view. For example, in the realm of graphics, a triangular prism could be interpreted as a compound of two quadrilateral projections or as a compound of one quadrilateral projection and one triangular projection. However, no ambiguities usually arise if three orthogonal 2-D projections are given. Likewise, no ambiguities usually exist in a mapping from 3-D to 2-D.

The principal intent of the present paper is to identify and resolve the ambiguities, if any, that arise while expressing steady-state 3-D helical chips in terms of the parameters η, ρ_s and ρ_u of two orthogonal 2-D views of the chip. As in [4,5], the analysis focuses on the fundamental case of machining with tools with flat rake faces. It would be difficult to study the chip forms obtained with complex chip formers if one does not have a clear understanding of the simpler case of cutting with flat rake face tools. Further, an equivalent flat rake face is often invoked in the analysis of cutting with complex chip formers.

It will be argued that there exist several plausible definitions of ρ_u and ρ_s depending on the chosen viewpoint concerning up-curl and side-curl components of a 3-D chip. A 3-D chip form analysis will be developed to identify the relationship corresponding to each definition between the parameter set (ρ, p and θ) of the 3-D chip form and the parameter set (ρ_u and η, ρ_s) of the two 2-D views of chip up-curl and side-curl. It will be shown that these relationships are distinct and the relationship presented in [4,5] seems to be just one of them. The alternative relationships will be compared to identify the most logical candidate(s).

2. Alternative plausible definitions of up-curl and side-curl radii

Consider the definitions adopted in [4,5] first. Fig. 1b is an adaptation of the illustration used by Nakayama and Arai [5] in defining the radii of up-curl (ρ_u) and side curl (ρ_s) while machining with a tool with a plane rake face. In this illustration, axis X is along the TCSL, axis Y is perpendicular to X while being parallel to the rake plane, and axis Z is perpendicular to both X and Y (i.e. perpendicular to the rake plane). The origin is set on axis X at the end cutting edge side of the chip. According to [5], "when the two circular arcs in the Fig. 1b are compounded, the helix in Fig. 1a is produced". The radius of the arc in plane YZ is then taken as the radius of up-curl, ρ_u, whereas the radius of the arc in plane XY is taken as the radius of side-curl, ρ_s.

The following characteristics of the pure forms of up-curl and side-curl are recognised in [4,5]:

- Pure up-curl: The TCSL is parallel to the cutting edge, i.e. $\Delta\psi = 0$. Hence the plane normal to the TCSL is identical to that normal to the cutting edge. Tool-chip contact length, l_c, chip velocity, $\mathbf{V}_c$, and ρ_u are uniform along the TCSL The chip axis is parallel to the rake plane, i.e. $\theta = 0$. Likewise, $\eta = 0$ and $\eta_c = 0$. The chip geometry is completely determined by considering just the plane normal to the cutting edge.

- Pure side-curl: $\mathbf{V}_c$ is linearly varying along the TCSL so that $\Delta\psi \neq 0$ and ρ_s is not constant along the TCSL. The chip axis is normal to the rake plane, i.e. $|\theta| = 90°$. The chip geometry is completely determined by considering just the tool rake plane (i.e. the plane XY).

Nakayama et al. [4,5] considered 3-D chip formation and assumed that plane YZ is the plane of up-curl and that the projections of velocity $\mathbf{V}_c$ of the chip particle on planes YZ and XY respectively match, as instantaneous linear velocities of rotations, the angular velocities of rotations with respect to up-curl and side-curl. Further, they noted that the angular velocity, $\boldsymbol{\omega}$, of the 3-D chip has only two non-zero components, $\boldsymbol{\omega}_x$ and $\boldsymbol{\omega}_z$, perpendicular to planes YZ and XY respectively. Hence they identified these as the angular velocities of up-curl in plane YZ and side-curl in plane XY respectively. Thus, the radii of up-curl and side-curl of 3-D chip were taken

to be the radii of rotation in planes YZ and XY respectively. This procedure led to expressions for ω_z and ω_x in the form of equations (N1) and (N2) listed in Table 1. These expressions were then utilised in relating to 3-D helical chip geometry to arrive at equations (N3) and (N4) for θ and ρ respectively. Note that, although Nakayama et al. [4,5] had not explicitly stated them, a combination and rearrangement of equations (N3) and (N4) leads to equations (N5) and (N6) for ρ_u and ρ_s respectively (see Table 1).

However, a deeper examination of the analysis of Nakayama et al. points to several potential inconsistencies. For instance, the analysis assumes that the angular velocity of pure up-curl lies *in* the plane XZ. Whereas, in the case of a 3-D chip, this angular velocity, $\boldsymbol{\omega}_x$, can lie in a plane which has a non-zero offset from plane XZ. Therefore a potential inconsistency exists with regard to equation (N2). Hence there is a need to define ρ_u and ρ_s in such a manner as to avoid inconsistencies when analysing 3-D chips. We then tried to find such definitions. However, it soon became clear that this can be done from several viewpoints. Firstly, one can adopt the viewpoint of rotation *or* that of curvature. Secondly, one can view them with reference to the TCSL (it will be shown later that the TCSL has to be straight and parallel to A_{Hr} if the chip is helical) *or* the chip velocity $\mathbf{V}_c$ (since, in the case of pure curl the plane normal to the TCSL is identical to the plane parallel to $\mathbf{V}_c$ and normal to the rake plane). Finally, one can consider them to be the components of the radius of chip particle rotation in the desired directions *or* the radii of the rotation components about the desired axes. This range of viewpoints may be captured in the six alternative sets of definitions of ρ_u and ρ_s described below.

Hypotheses concerning the definitions of ρ_u and ρ_s:

1. $\boldsymbol{\rho}_u$ is the component of the position vector $\boldsymbol{\rho}$ (the radius vector of rotation of chip particle at point O around chip axis) in the direction normal to the tool rake plane. $\boldsymbol{\rho}_s$ is the remaining component of $\boldsymbol{\rho}$ parallel to the rake plane.

Table 1
Equations developed or implied by Nakayama et al. [4,5]

Equation No.	Note	Equation
N1	[4]	$\omega_z = V_c/\rho_s$
N2	[4]	$\omega_x = (V_c\cos\eta)/\rho_u$
N3	[4,5]	$\tan\theta = \omega_z/\omega_x = \rho_u/(\rho_s\cos\eta)$
N4	[4,5]	$\rho = \sqrt{\dfrac{1 - \sin^2\eta\cos^2\theta}{(\cos\eta/\rho_u)^2 + (1/\rho_s)^2}}$
N5	By combining N3 and N4	$\rho_u = \dfrac{\rho\cos\eta}{\cos\theta\sqrt{1 - \sin^2\eta\cos^2\theta}}$
N6	By combining N3 and N4	$\rho_s = \dfrac{\rho}{\sin\theta\sqrt{1 - \sin^2\eta\cos^2\theta}}$

2. ρ_u is the radius of rotation of chip particle at point O around the axis directed parallel to A_{Hr} (TCSL). ρ_s is the radius of the corresponding rotation about the axis directed normal to the rake plane.
3. ρ_u is the radius of curvature of the chip helix at point O in the direction normal to the rake plane. ρ_s is the radius of the remaining curvature in a direction parallel to the rake plane.
4. ρ_u is the radius of curvature at point O of the projection of the chip helix on a plane normal to A_{Hr} (TCSL). ρ_s is the corresponding radius of curvature of the projection of the chip helix on the rake plane.
5. ρ_u is the radius of rotation of point O around the axis directed normal to the chip velocity vector $\mathbf{V}_c$ while being parallel to the rake plane. ρ_s is the radius of the corresponding rotation about the axis directed normal to the rake plane.
6. ρ_u is the radius of curvature at point O of the projection of the chip helix on the plane parallel to the chip velocity $\mathbf{V}_c$ while being normal to the rake plane. ρ_s is the corresponding radius of curvature of the projection of the chip helix on the rake plane.

The next section will determine the expressions for the various parameters that equate to ρ_u and ρ_s respectively following the six alternative hypotheses in terms of the geometric parameters (ρ, θ, and η) of the generalised 3-D helical chip. The analysis will also identify the 3rd radius component, ρ_3, if it exists in view of the 3-D nature of the mixed chip.

3. Geometric analysis of 3-D helical chip

Fig. 3 illustrates the geometric analysis. In contrast to [4,5], where it was assumed that the TCSL is a straight-line segment, we will start with the assumption that the TCSL is a plane curve. The right-handed Cartesian system XYZ is centred at an arbitrary point, O, on the TCSL. Axis Z is normal to the rake plane, P_r, with the positive direction outward from the tool rake face (as in [4,5]). Axis Y is normal to the projection, A_{Hr}, of the chip helix axis, A_H, on P_r and is directed towards the right as shown in Fig. 3 (a generalised definition of the direction of Y will be provided in Part 2). Note that axes X and Y lie on P_r. In Fig. 3, O_0OO_1 is the TCSL which is initially assumed to be curved. The outer surface of the chip is generated due to the helical motion of the TCSL about axis A_H. Thus, points O_0 and O_1 are the boundary points on the TCSL that generate helix $\mathbf{H}_0$ with radius ρ_0 and helix $\mathbf{H}_1$ with radius ρ_1 respectively. The convention adopted is that $\rho_0 > \rho_1$. This means that when $\rho_0 = \rho_1$ (as in the case of a tubular helical chip), the choice of points O_0 and O_1 becomes uncertain. However, either choice would lead to the same chip form parameters.

$\mathbf{V}_c$ is the velocity of the chip particle at O, which should lie on the tool rake plane [4]. Let η be the angle between $\mathbf{V}_c$ and axis Y. A trajectory of the chip particle starting at point O is a circular helix, **H**. Hence $\mathbf{V}_c$ can be resolved into two orthogonal instantaneous velocities $\mathbf{V}_T$ and $\mathbf{V}_R$: $\mathbf{V}_T$ is the translational velocity parallel to the helix axis, A_H, and $\mathbf{V}_R$ is the rotational velocity corresponding to the angular velocity of rotation, $\boldsymbol{\omega}$, about A_H. A steady state chip implies a

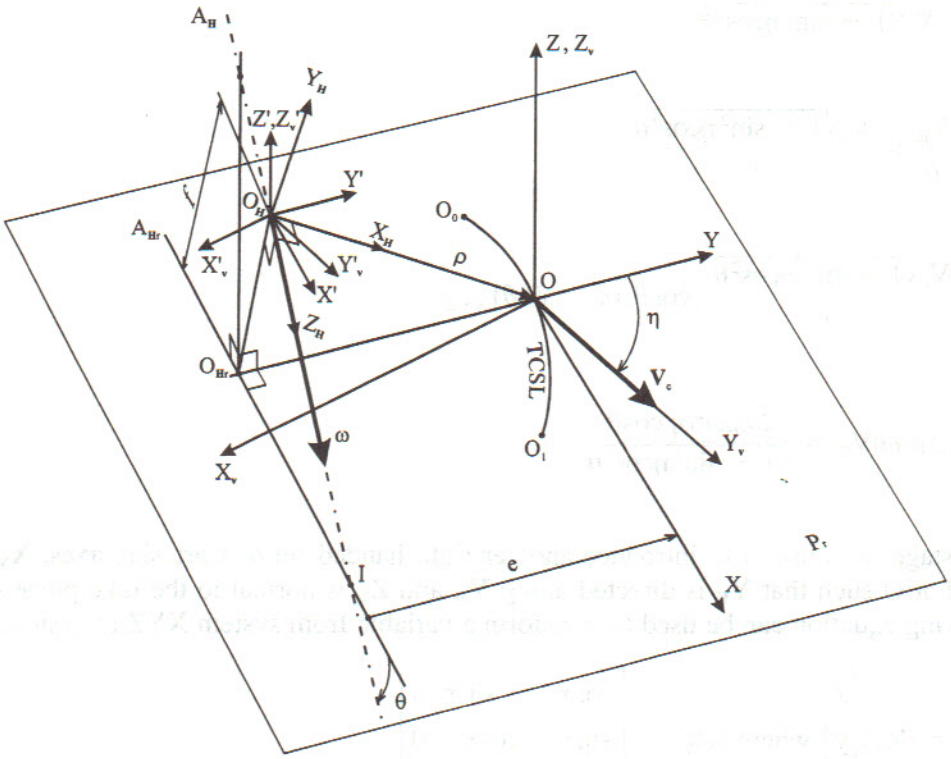

Fig. 3. Geometric analysis of 3-D helical chip forms.

TCSL that remains constant in space and time. The analysis in Part 1 will mainly present the expressions for various important parameters related to point O of the TCSL, i.e. to helix **H**. The analysis will be extended in Part 2 to the entire chip, i.e. to helices $\mathbf{H}_0$ and $\mathbf{H}_1$.

The following equations can now be progressively obtained from the above scenario:

$$\mathbf{V}_c = V_c\{\sin\eta, \cos\eta, 0\}_{XYZ} \tag{1}$$

$$\mathbf{V}_c = \mathbf{V}_R + \mathbf{V}_T \tag{2}$$

$$V_T = V_c \sin\eta\cos\theta \tag{3}$$

$$\mathbf{V}_T = V_c \sin\eta\cos\theta\{\cos\theta, 0, -\sin\theta\}_{XYZ} \tag{4}$$

$$\mathbf{V}_R = \mathbf{V}_c - \mathbf{V}_T = V_c\{\sin\eta\sin^2\theta, \cos\eta, \sin\eta\sin\theta\cos\theta\}_{XYZ} \tag{5}$$

$$V_R = V_c\sqrt{1 - \sin^2\eta\cos^2\theta} \tag{6}$$

$$\omega = \frac{V_R}{\rho} = \frac{V_c\sqrt{1 - \sin^2\eta\cos^2\theta}}{\rho} \tag{7}$$

$$\omega = \frac{V_c\sqrt{1 - \sin^2\eta\cos^2\theta}}{\rho}\{\cos\theta, 0, -\sin\theta\}_{XYZ} \tag{8}$$

$$p = (2\pi/\omega)V_T = \frac{2\pi\rho\sin\eta\cos\theta}{\sqrt{1 - \sin^2\eta\cos^2\theta}} \tag{9}$$

At this stage, it is useful to introduce another right handed set of Cartesian axes, X_V, Y_V, and Z_V centred at O such that Y_V is directed along $\mathbf{V}_c$, and Z_V is normal to the rake plane ($Z_V \equiv Z$). The following equation can be used to transform a variable from system XYZ to system $X_VY_VZ_V$:

$$\begin{Bmatrix} x_v \\ y_v \\ z_v \end{Bmatrix} = [\mathbf{R_V}]\begin{Bmatrix} x \\ y \\ z \end{Bmatrix} \text{ where } [\mathbf{R_V}] = \begin{bmatrix} \cos\eta & -\sin\eta & 0 \\ \sin\eta & \cos\eta & 0 \\ 0 & 0 & 1 \end{bmatrix} \tag{10}$$

Let O_H be the point on A_H such that line OO_H is perpendicular to A_H. Clearly, the position vector (or the radius vector), $\boldsymbol{\rho}$, of the helix generated by point O has a magnitude equal to distance O_HO and is directed along O_HO. Let $\mathbf{u}_\rho$, $\mathbf{u}_{V_R}$, and $\mathbf{u}_\omega$ be the unit vectors directed along $\boldsymbol{\rho}$, $\mathbf{V}_R$ and $\boldsymbol{\omega}$ respectively. Then $\mathbf{u}_\rho$ must be directed normal to $\mathbf{u}_{V_R}$ as well $\mathbf{u}_\omega$ because $\mathbf{V}_R = \boldsymbol{\omega} \times \boldsymbol{\rho}$. Thus,

$$\begin{aligned} \boldsymbol{\rho} &= \rho\mathbf{u}_\rho = \rho(\mathbf{u}_{V_R} \times \mathbf{u}_\omega) = (\mathbf{V}_R \times \omega)/\omega^2 \\ &= \frac{\rho}{\sqrt{1 - \sin^2\eta\cos^2\theta}}\{-\cos\eta\sin\theta, \sin\eta\sin\theta, -\cos\eta\cos\theta\}_{XYZ} \\ &= \frac{\rho}{\sqrt{1 - \sin^2\eta\cos^2\theta}}\{-\sin\theta, 0, -\cos\eta\cos\theta\}_{X_vY_vZ_v} \end{aligned} \tag{11}$$

Let O_{Hr} be the projection of O on A_{Hr}. Let e and f be the distances $O_{Hr}O$ and O_HO_{Hr} respectively. It can be shown from Fig. 3 that

$$e = \rho_y = \frac{\rho\sin\eta\sin\theta}{\sqrt{1 - \sin^2\eta\cos^2\theta}} = \frac{V_T\tan\theta}{\omega} \tag{12}$$

$$f = \frac{\rho\cos\eta}{\sqrt{1 - \sin^2\eta\cos^2\theta}} \tag{13}$$

If it is assumed that the chip is in steady state helical motion as a rigid body after leaving the TCSL, every helix on the chip must have the same $\mathbf{V}_T$ and $\boldsymbol{\omega}$. Applying the conditions of constancy of $\mathbf{V}_T$, ω, and θ to Eq. (12), it follows that the magnitude of e must be the same for every point on TCSL. This implies that (i) the TCSL must be a straight-line segment, and (ii) the segment must be parallel to A_{Hr}. Hence the TCSL has to be a straight-line segment collinear with axis X.

Recall that point O_0 generates the chip helix with the largest radius whereas point O_1 generates the helix with the smallest radius. If we locate O_0 at the end cutting edge side of chip and O is taken to represent O_0 (which generates the outer helix), then our axes X, Y, Z (Fig. 3) will coincide with axes X, Y, Z used in [4,5]. Otherwise, point O should be taken to represent point O_1 (generating the inner helix) to obtain coincidence between the two coordinate systems. It is therefore evident that the Cartesian axes used in [4,5] do not always correspond to the outer or inner helix of the chip. Hence, for two chips with geometrically identical screw faces, the estimates of up-curl and side-curl radii resulting from the analysis in [4,5] can differ significantly depending on whether the axis system happened to be centred on the inner or the outer helix of the screw surface of the chip.

It is now possible to develop expressions for estimating ρ_u and ρ_s and the corresponding 3rd radius component of chip curling (if it exists) following hypotheses 1 to 6.

- Hypothesis 1:

Utilising Eq. (11)

$$\rho_u = \rho_z = \rho_{z_v} = \frac{-\rho\cos\eta\cos\theta}{\sqrt{1 - \sin^2\eta\cos^2\theta}} \tag{14a}$$

$$\rho_s = \sqrt{\rho_x^2 + \rho_y^2} = \sqrt{\rho_{x_v}^2 + \rho_{y_v}^2} = \frac{-\rho\sin\theta}{\sqrt{1 - \sin^2\eta\cos^2\theta}} \tag{14b}$$

- Hypothesis 2:

This hypothesis requires the consideration of axes X′, Y′, and Z′, which are parallel to axes X, Y, and Z respectively while being centred at O_H. It can be shown that the radius of rotation, $\rho^{\omega x'}$, of point O about axis X′ is equal to $\sqrt{\rho_y^2 + \rho_z^2}$ and hence

$$\rho_u = \rho^{\omega x'} = \sqrt{\rho_y^2 + \rho_z^2} = \rho\sqrt{\frac{\cos^2\eta\cos^2\theta + \sin^2\eta\sin^2\theta}{1 - \sin^2\eta\cos^2\theta}} \tag{15a}$$

Following similar arguments,

$$\rho_s = \rho^{\omega_{Z'}} = \sqrt{\rho_x^2 + \rho_y^2} = \frac{\rho\sin\theta}{\sqrt{1 - \sin^2\eta\cos^2\theta}} \tag{15b}$$

$$\rho_3 = \rho^{\omega_{Y'}} = \sqrt{\rho_z^2 + \rho_x^2} = \frac{\rho\cos\eta}{\sqrt{1 - \sin^2\eta\cos^2\theta}} \tag{15c}$$

- Hypothesis 3:

This hypothesis requires the vector of curvature, $\boldsymbol{\kappa}$, of helix **H** to be determined at point O. With a view to identifying the equation of **H**, we may define an intrinsic coordinate system $X_H Y_H Z_H$ centred at O such that X_H is directed as $\mathbf{u}_\rho$ (i.e. in the direction O_H to O), Z_H is directed as $\mathbf{u}_\omega$ (along the helix axis), and Y_H is chosen such that $X_H Y_H Z_H$ is a right-handed orthogonal triplet. The helical path **H** can then be expressed as a function of time t (taking t = 0 when the chip particle is at O) as

$$\mathbf{H}(t) = \{\rho\cos\omega t, \rho\sin\omega t, V_T t\}_{X_H Y_H Z_H} \tag{16}$$

The above equation for **H** may be transformed to the coordinate system XYZ by utilising the following transformation equation derivable from the geometry of Fig. 3:

$$\begin{Bmatrix} x \\ y \\ z \end{Bmatrix} = [\mathbf{R_H}]\begin{Bmatrix} x_H \\ y_H \\ z_H \end{Bmatrix} + \begin{Bmatrix} f\sin\theta \\ -e \\ f\cos\theta \end{Bmatrix} \tag{17a}$$

where

$$[\mathbf{R_H}] = \begin{bmatrix} \dfrac{-\cos\eta\sin\theta}{\sqrt{1 - \sin^2\eta\cos^2\theta}} & \dfrac{\sin\eta\sin^2\theta}{\sqrt{1 - \sin^2\eta\cos^2\theta}} & \cos\theta \\ \dfrac{\sin\eta\sin\theta}{\sqrt{1 - \sin^2\eta\cos^2\theta}} & \dfrac{\cos\eta}{\sqrt{1 - \sin^2\eta\cos^2\theta}} & 0 \\ \dfrac{-\cos\eta\cos\theta}{\sqrt{1 - \sin^2\eta\cos^2\theta}} & \dfrac{\sin\eta\sin\theta\cos\theta}{\sqrt{1 - \sin^2\eta\cos^2\theta}} & -\sin\theta \end{bmatrix} \tag{17b}$$

Next, applying well-known principles of helical geometry, it can be shown that

$$\boldsymbol{\kappa} = (1/\rho)\sqrt{1 - \sin^2\eta\cos^2\theta}\{\cos\eta\sin\theta, -\sin\eta\sin\theta, \cos\eta\cos\theta\}_{XYZ} \tag{18}$$

and thus

$$\kappa = |\boldsymbol{\kappa}| = \frac{1 - \sin^2\eta\cos^2\theta}{\rho} \tag{19}$$

Therefore, following Hypothesis 3,

$$\rho_u = \frac{1}{\kappa_z} = \frac{1}{\kappa_{z_v}} = \frac{\rho}{\cos\eta\cos\theta\sqrt{1 - \sin^2\eta\cos^2\theta}} \tag{20a}$$

$$\rho_s = \frac{1}{\sqrt{\kappa_x^2 + \kappa_y^2}} = \frac{1}{\sqrt{\kappa_{x_v}^2 + \kappa_{y_v}^2}} = \frac{\rho}{\sin\theta\sqrt{1 - \sin^2\eta\cos^2\theta}} \tag{20b}$$

- Hypothesis 4:

Applying the transformation represented by Eq. (17a) and (17b) to the definition of helix **H** given by Eq. (16), it is a straight forward exercise to determine the projections $\mathbf{H}^{xy}$, $\mathbf{H}^{yz}$ and $\mathbf{H}^{zx}$ of **H** on planes XY, YZ, and ZX respectively and then to determine the corresponding radii of curvature $\rho_{\mathbf{H}xy}$, $\rho_{\mathbf{H}yz}$ and $\rho_{\mathbf{H}zx}$ respectively at time t = 0, i.e. when the chip particle is at point O. Thus, Hypothesis 4 implies that

$$\rho_u = \rho_{\mathbf{H}yz}|_{t=0} = \frac{\rho\cos\eta}{\cos\theta\sqrt{1 - \sin^2\eta\cos^2\theta}} \tag{21a}$$

$$\rho_s = \rho_{\mathbf{H}xy}|_{t=0} = \frac{\rho}{\sin\theta\sqrt{1 - \sin^2\eta\cos^2\theta}} \tag{21b}$$

$$\rho_3 = \rho_{\mathbf{H}zx}|_{t=0} = \frac{\rho\sin^2\eta}{\cos\eta\cos\theta\sqrt{1 - \sin^2\eta\cos^2\theta}} \tag{21c}$$

- Hypothesis 5:

This hypothesis requires a procedure similar to that used for Hypothesis 2 with the exception that, instead of considering the radii of rotation around axes X′, Y′, and Z′, we consider radii of rotation around axes X_v', Y_v', and Z_v' which are parallel to axes X_v, Y_v, and Z_v respectively. Hence, it can be shown that

$$\rho_u = \rho^{\omega_{X_v'}} = \frac{\rho\cos\eta\cos\theta}{\sqrt{1 - \sin^2\eta\cos^2\theta}} \tag{22a}$$

$$\rho_s = \rho^{\omega_{Z_v'}} = \frac{\rho\sin\theta}{\sqrt{1 - \sin^2\eta\cos^2\theta}} \tag{22b}$$

$$\rho_3 = \rho^{\omega_{Y_v'}} = \rho \tag{22c}$$

• Hypothesis 6:

This hypothesis requires a procedure similar to that used for Hypothesis 4 with the exception that, instead of evaluating the curvatures at O of projections $\mathbf{H}^{xy}$, $\mathbf{H}^{yz}$ and $\mathbf{H}^{zx}$ with reference to the system XYZ, we determine the radii of curvature $\rho_{\mathbf{H}x_vy_v}$, $\rho_{\mathbf{H}y_vz_v}$, $\rho_{\mathbf{H}y_vz_v}$ of projections $\mathbf{H}^{x_vy_v}$, $\mathbf{H}^{y_vz_v}$ and $\mathbf{H}^{z_vx_v}$ respectively. Thus,

$$\rho_u = \rho_{\mathbf{H}y_vz_v}|_{t=0} = \frac{\rho}{\cos\eta\cos\theta\sqrt{1-\sin^2\eta\cos^2\theta}} \tag{23a}$$

$$\rho_s = \rho_{\mathbf{H}x_vy_v}|_{t=0} = \frac{\rho}{\sin\theta\sqrt{1-\sin^2\eta\cos^2\theta}} \tag{23b}$$

$$\rho_3 = \rho_{\mathbf{H}z_vx_v}|_{t=0} = \frac{0}{0} \tag{23c}$$

Although ρ_3 is indeterminate according to Eq. (23c), by considering the expression

$$\rho_3 = \rho_{\mathbf{H}z_vx_v}|_{t\to 0} \tag{23d}$$

one finds that

$$\rho_3 = 0 \tag{23e}$$

4. Validation of the hypotheses

The following six criteria are believed to be necessary and sufficient for the complete validation of each hypothesis.

From considerations of pure up-curl, i.e. when one substitutes $\eta = 0$ and $\theta = 0$ in the expressions for ρ_u and ρ_s, one should find that:

Criterion 1: $|\rho_u| = \rho$ Criterion 2: $|\rho_s| = \infty$.

From considerations of pure side-curl, i.e. when one substitutes $\theta = -90°$ or $90°$ in the expressions for ρ_u and ρ_s, one should find that:

Criterion 3: $|\rho_s| = \rho$ Criterion 4: $|\rho_u| = \infty$.

ρ_u and ρ_s together should be sufficient to fully account in 3-D the viewpoint from which they have been defined, i.e. rotation or curvature. This expectation leads to the following two additional criteria:

Criterion 5 (completeness): Either ρ_3 does not exist at all, or has zero magnitude if the definition

is based on the viewpoint of rotation or has infinite magnitude if the viewpoint is based on curvature.

Criterion 6 (orthogonality):

If the hypothesis defines ρ_u and ρ_s from the viewpoint of rotation, *then* $\sqrt{\rho_u^2 + \rho_s^2}$ must be equal to ρ;

If the hypothesis defines ρ_u and ρ_s from the viewpoint of curvature, *then* $\sqrt{\frac{1}{\rho_u^2} + \frac{1}{\rho_s^2}}$ must be equal to κ (ref. to Eq. (19)).

Table 1 summarises the results obtained from the application of the above six criteria to the six hypotheses.

5. Discussion

It is seen from Table 2 that only Hypothesis 3 has satisfied all the six criteria. This hypothesis is based on the viewpoint of chip helix curvature and utilises the rake plane orientation as the reference. The definitions of ρ_u and ρ_s are such that the same expressions for them are obtained

Table 2
Validation of the hypotheses concerning the definitions of ρ_u and ρ_s

Hypothesis	Viewpoint	Reference	See Eq.	Is the criterion satisfied?					
				1	2	3	4	5	6
1	Rotation, components of radius of rotation	Rake plane	14a, b	Yes	No	Yes	No	Yes	Yes
2	Rotation, radii of components of rotation	A_{Hr} or TCSL	15a, b, c	Yes	No	Yes	No	No	No
3	Curvature, radii of curvature components	Rake plane	20a, b	Yes	Yes	Yes	Yes	Yes	Yes
4*	Curvature, radii of curvature of projections	A_{Hr} or TCSL	21a, b, c	Yes	Yes	Yes	Yes	No	No
5	Rotation, radii of components of rotation	Chip velocity $\mathbf{V}_c$	22a, b, c	Yes	No	Yes	No	No	No
6	Curvature, radii of curvature of projections	Chip velocity $\mathbf{V}_c$	23a, b, e	Yes	Yes	Yes	Yes	No	No

*The expressions for ρ_u and ρ_s are identical to those implied by [4,5].

whether one analyses with reference to A_{Hr} (or the TCSL) or chip velocity V_c. The generalised 3-D expressions satisfy the specific conditions of both the 2-D cases: pure up curl and pure side curl (criteria 1–4). The third radius component, ρ_3, does not exist (criterion 5). Finally ρ_u and ρ_s together suffice to fully account for the total chip helix curvature (criterion 6).

The identification and validation of Hypothesis 3 is the main new and positive finding of the present work. Combining Hypothesis 3 (Eq. (20a) and (20b)) with Eq. (8), it can be shown that

$$\omega_z = \frac{V_c}{\rho_s} \tag{24}$$

$$\omega_x = \frac{V_c}{\rho_u \cos\eta} \tag{25}$$

$$\tan\theta = \omega_z/\omega_x = (\rho_u \cos\eta)/\rho_s \tag{26}$$

$$\rho = \sqrt{\frac{1 - \sin^2\eta\cos^2\theta}{\{1/(\rho_u\cos\eta)\}^2 + (1/\rho_s)^2}} \tag{27}$$

Note that although Hypothesis 6 does not satisfy criterion 5 concerning ρ_3 it leads to expressions for ρ_u and ρ_s (see Eq. (23a) and (23b)) that are identical to Eq. (20a) and (20b) respectively derived from Hypothesis 3. This observation suggests that, as far as the estimation of the values of ρ_u and ρ_s that are in agreement with those derived from Hypothesis 3 is concerned, one can take the value of ρ_u to be equal to the value of the radius of the curvature of the projection of the chip helix on a plane containing the chip velocity vector while being normal to the rake plane, likewise the value of ρ_s to be equal to the value of a similar parameter estimated from the projection on the tool rake plane.

The equations for ρ_u and ρ_s (see Eq. (21a) and (21b)) derived from Hypothesis 4 are identical to equations (N5) and (N6) respectively implied by Nakayama et al. [4,5]. This observation suggests that the same values of ρ_u and ρ_s as derivable from [4,5] are obtained if one takes ρ_u to be the curvature of the projection of the chip helix on a plane perpendicular to the TCSL while being normal to the rake plane and ρ_s to be a similar parameter estimated from the projection on the rake plane. However, Hypothesis 4 has to be rejected because it does not satisfy criteria 5 and 6. In fact, Nakayama et al. [4,5] had not addressed the issue of the existence of a third radius component, ρ_3 (see criterion 5). One may therefore simplistically argue that the equations for ρ_u and ρ_s implied by their analysis *could* satisfy criterion 5. However, in fact, ρ_3 does exist as it follows when equations (N5) and (N6) are examined against criterion 6 from all plausible viewpoints (curvature and rotation) concerning the definitions of the radii. In other words, the magnitudes of ρ_u and ρ_s as obtained from equations (N5) and (N6) would not in general be adequate to fully account for the radius of total curvature or rotation. This leads us to the negative finding that the analysis of Nakayama et al. [4,5] yields an inadmissible system of expressions for ρ_u and ρ_s.

It may be also noted that the expressions derived by Nakayama et al. for ω_z and ρ_s (see equations (N1) and (N6)) are identical to those derived from the previously validated Hypothesis 3 (see Eqs. (24) and (20b)). However, there are significant differences in the expressions for ω_x, $\tan\theta$, ρ, and ρ_u derived from the two analyses. Comparing equations (N2) to (N5) of Nakayama et al. with Eqs. (25)–(27) and (20a) respectively, it is seen that the differences lie in the locations of the "cosη" terms. Thus, the analysis of Nakayama et al. [4,5] does yield fairly accurate estimates of ρ_u when angle η is small (i.e. $\cos\eta \approx 1$). Further, when the side-curl component is dominant in a mixed chip (i.e. $|\theta|$ is large), the magnitude of $|\eta|$ at point O_1 (i.e. that of $|\eta_1|$) can become very large. In particular, in pure side-curl, $|\eta_1|$ can reach 90°. Hence, it is interesting to examine the behaviour of Eq. (20a) and (N5) when $\eta = \theta = -90°$ and 90°. When one does this it is found that Eq. (20a) yields the expected infinite magnitude for ρ_u whereas equation (N5) yields an *indeterminate* value. Therefore the major weakness of the analysis of Nakayama et al. lies in the modelling of up-curl radius, ρ_u.

Consider now the plane of up-curl as implied by Hypothesis 3. The hypothesis takes the tool rake plane to be the plane of side-curl. The component of total curl curvature, $\boldsymbol{\kappa}$, chosen for the definition of ρ_u is $\boldsymbol{\kappa}_z$ which lies in the plane normal to the rake plane. The corresponding component chosen for the definition of ρ_s is $\boldsymbol{\kappa}_x + \boldsymbol{\kappa}_y$ which is inclined at angle η to axis X as can be easily determined from Eq. (18). Hence, $\boldsymbol{\kappa}_x + \boldsymbol{\kappa}_y$ is normal to the chip velocity $\mathbf{V}_c$. In other words, the plane passing through chip velocity, $\mathbf{V}_c$, while being orthogonal to the rake plane is the unique plane which contains $\boldsymbol{\kappa}_z$ and is orthogonal to $\boldsymbol{\kappa}_x + \boldsymbol{\kappa}_y$. Consequently it this plane (X_VZ_V), but not plane YZ as assumed in the analysis of Nakayama et al. [4,5], that should be taken as the plane of up-curl.

The following final picture concerning the mapping between 3-D and 2-D views of chip form emerges from the above analysis and discussion:

- The central idea of *reconstructing* the 3-D chip helix in terms of the parameters of two orthogonal 2-D views representing up-curl and side-curl respectively is reasonable. However it is not possible to define the radii of up-curl and side-curl such that they are compatible with their 2-D definitions and, when applied to 3-D chips, enable the simultaneous reconstruction of the rotation as well as the curvature of the chip. This is because the angular velocity of total rotation lies in a plane parallel to plane XZ whereas the vector of total curvature lies in plane X_VZ_V. Hence a choice needs to be made between the viewpoints of rotation and curvature. The rotational viewpoint was chosen in [4,5]. The present work shows that the curvature viewpoint is the more logical choice.
- In pure side-curl, chip rotation as well as chip curvature occur within the tool rake plane. The same is true in the case of 3-D chips. Therefore no ambiguities exist with regard to the definition of side-curl. Hence equation (N6) for ρ_s implied by [4,5] is identical to Eq. (20b) derived in the present work.
- In pure up-curl, chip rotation as well as curvature occurs in a plane normal to the tool rake plane. However, two alternative definitions of such a normal plane are plausible: (i) plane XZ which is normal to the TCSL, or (ii) plane X_VZ_V which is parallel to $\mathbf{V}_c$. Nakayama et al. [4,5] had chosen plane XZ. This choice is acceptable as far as the reconstruction of the total angular velocity of rotation of the 3-D chip is concerned since the total angular velocity can indeed be resolved into two components parallel to planes XY and YZ. However, the choice is not

acceptable while reconstructing the radius of rotation since there exists a 3rd radius component orthogonal to ρ_u and ρ_s that remains unaccounted for (see criterion 6 and Hypothesis 2).

- No inconsistencies however arise if one chooses the viewpoint of curvature and takes up-curl to be occurring in the plane $X_V Z_V$. The only way to completely decompose the total curvature of a 3-D chip helix into two orthogonal components such that one of these (i.e. side-curl) lies in a plane parallel to the tool rake plane (i.e. plane $Y_V Z_V$) is to choose the other component (up-curl) to lie in a plane parallel to plane $X_V Y_V$. The radii of up-curl and side-curl thus obtained are able to completely reconstruct the radius of total curvature of the 3-D chip helix. This unique ability of complete reconstruction is achieved by Hypothesis 3. Therefore, Eq. (20a) and (20b) derived from Hypothesis 3 represent the most logical choices for estimating the magnitudes ρ_u and ρ_s corresponding to a given 3-D chip.

6. Conclusions

A basic 3-D analysis of the geometry of chip forms has been developed with a view to determining the relationship between the geometry of steady-state 3-D helical chips and the 2-D concepts of pure up-curl and pure side-curl. Six hypotheses have been identified concerning the definitions of the radii of up-curl and side-curl, i.e. ρ_u and ρ_s respectively. These hypotheses have been tested against six criteria. The analysis has led to the following conclusions:

1. The tool-chip separation line must be a straight-line segment when the tool rake face is flat and the chip is in steady state helical motion as a rigid body after leaving the tool-chip separation line.
2. Hypothesis 3, which has been developed from the viewpoint of chip curvature with specific reference to the chip velocity direction, is the most logical one to be adopted in relating the 2-D concepts of pure up-curl and pure side-curl to the geometry of 3-D helical forms generally obtained in practice. Eq. (20a) and (20b) enable the determination of the radii of pure up-curl and pure side-curl respectively from given magnitudes of parameters θ, ρ, and η of 3-D helical chips.
3. The prevailing notions concerning the estimation of the radii of pure up-curl and side-curl from 3-D chip forms, which have been pioneered by Nakayama et al. [4,5], lead to some unsatisfactory results. While their expression for the radius of side-curl is correct, there is significant error in the expression for the radius of up-curl. The errors associated with the application of their analysis increase with increasing magnitude of $|\eta|$.

References

[1] P.K. Venuvinod, A. Djordjevich, Towards Active Chip Control, Annals of the CIRP 45 (1) (1995) 83–86.
[2] C. Spaans, The fundamentals of three-dimensional chip curl, chip breaking and chip control, PhD thesis, TH-Delft, 1971.
[3] ISO 3685: Tool-life testing with single-point turning tools, Annex G, 1977:41.

[4] K. Nakayama, M. Ogawa, Basic Rules on the Form of Chip in Metal Cutting, Annals of the CIRP 27 (1) (1978) 17–21.
[5] K. Nakayama, M. Arai, Comprehensive Chip Form Classification Based on the Cutting Mechanism, Annals of the CIRP 41 (1) (1992) 71–74.